JOURNAL OF MATERIALS SCIENCE 26 (1991) 5101–5106

Formation of the high-T_c phase in lead-doped Bi–Sr–Ca–Cu–O superconductors

KI HYUN YOON, HAE BUM LEE
Department of Ceramic Engineering, Yonsei University, Seoul, Korea

The characteristics of Bi–Sr–Ca–Cu–O superconductors have been investigated as a function of the amount of Pb addition. The volume fraction of the high-T_c phase increases with increasing Pb addition up to $x = 0.3$ in $(Bi_{1-x}Pb_x)_2Sr_2Ca_2Cu_3O_y$ and above that it decreases. The grain size is increased and density is decreased with increasing Pb addition, due to two-dimensional grain growth which results from formation of the high-T_c phase. The specimen with $x = 0.3$ has a transition temperature of 104 K and high magnetic susceptibility due to the fact that most of the volume fraction is of the high-T_c phase. Pb addition cause formation of Ca_2PbO_4 as a secondary phase and it produces a partially melted liquid phase below the sintering temperature, which acts as a flux and promotes formation of the high-T_c phase.

1. Introduction

Recently, Maeda *et al.* [1] discovered a new high-T_c oxide superconductor in the Bi–Sr–Ca–Cu–O system. It has been clarified that there are two superconducting phases with transition temperatures of 105 K (high-T_c phase) and 75 K (low-T_c phase). The former phase has a longer c axis than the latter phase. Much effort has been made to single out the high-T_c phase. Coexistence of the high-T_c phase with the low-T_c phase or semiconducting phase, however, has always been observed in this system. Thus, it has not been possible to obtain zero resistivity above 100 K although the onset of a resistive drop was observed even at 110 K. In order to increase the high-T_c phase, the addition of excess Ca and Cu [2, 3], prolonged sintering [4], low-temperature annealing [5] and low oxygen partial pressure sintering [6] have been attempted. Among these efforts, partial substitution of Pb in Bi–Sr–Ca–Cu–O superconductors was reported to be effective in increasing the proportion of the high-T_c phase [7]. After this, many researchers succeeded in obtaining samples with zero resistance states above 100 K [8, 9] and found that Pb substitution resulted in the stabilization of the high-T_c phase [10–12]. In this report, we investigate the change in proportion of the high-T_c phase, density, microstructure, magnetic susceptibility, transition temperature, and electrical properties of $(Bi_{1-x}Pb_x)_2Sr_2Ca_2Cu_3O_y$ high-T_c superconductors in the range from $x = 0$ to $x = 0.5$. We also discuss the formation mechanism of the high-T_c phase in relation to the second phase in the Pb-doped sample.

2. Experimental procedure

The powders were prepared with nominal compositions represented by $(Bi_{1-x}Pb_x)_2Sr_2Ca_2Cu_3O_y$ with $x = 0$ to $x = 0.5$ Pb through solid-state reactions of the appropriate amounts of Bi_2O_3, PbO, $SrCO_3$, $CaCO_3$ and CuO. Mixing was carried out in a mortar grinder by the wet method using ethyl alcohol for 24 h. The well-ground mixtures were calcined in air at 800 °C for 15 h, and after grinding the powders, these materials were again calcined in air at 840 °C for 15 h. The reacted powders were reground thoroughly and then pressed into pellets under a pressure of 5 t cm^{-2} to a diameter of 11 mm and thickness 3 mm and these were sintered in air for 75 h at 845 °C. The sintered pellets were cooled to room temperature in the furnace. The resultant phases were determined using an X-ray powder diffractometer with CuK_α radiation in the 2θ range from 3 to 60°. Differential thermal analysis (DTA) and thermogravimetric analysis (TGA) were employed to investigate the reaction composition of the calcined $(Bi_{1-x}Pb_x)_2Sr_2Ca_2Cu_3O_y$ powders. Scanning electron microscopy (SEM) was used to observe microstructure and energy-dispersive X-ray spectroscopy (EDS) to investigate the phases formed. The electrical resistivity was measured by the standard four-probe method for bar-shaped samples cut from the sintered pellets over a range of temperature from 50 to 300 K.

3. Results and discussion

Fig. 1 shows X-ray diffraction patterns of the $(Bi_{1-x}Pb_x)_2Sr_2Ca_2Cu_3O_y$ compositions with $x = 0$ to 0.5. For the $x = 0$ composition, almost all the peaks observed were peaks of the low-T_c phase. However, the peak intensities of the low-T_c phase decreased and conversely that of the high-T_c phase grew drastically with increase in the Pb doping amount, so a nearly single-phase pattern for the high-T_c phase was observed for the $x = 0.2$ and 0.3 compositions. The peak

0022–2461/91 $03.00 + .12

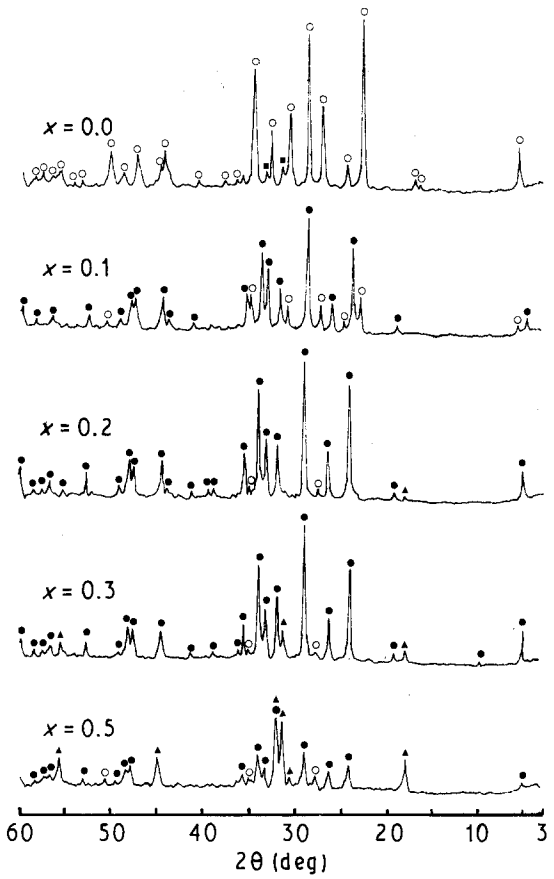

Figure 1 XRD patterns of $(Bi_{1-x}Pb_x)_2Sr_2Ca_2Cu_3O_y$: (○) low-$T_c$ phase, (●) high-T_c phase, (▲) Ca_2PbO_4, (■) $(Sr,Ca)_3Cu_5O_8$.

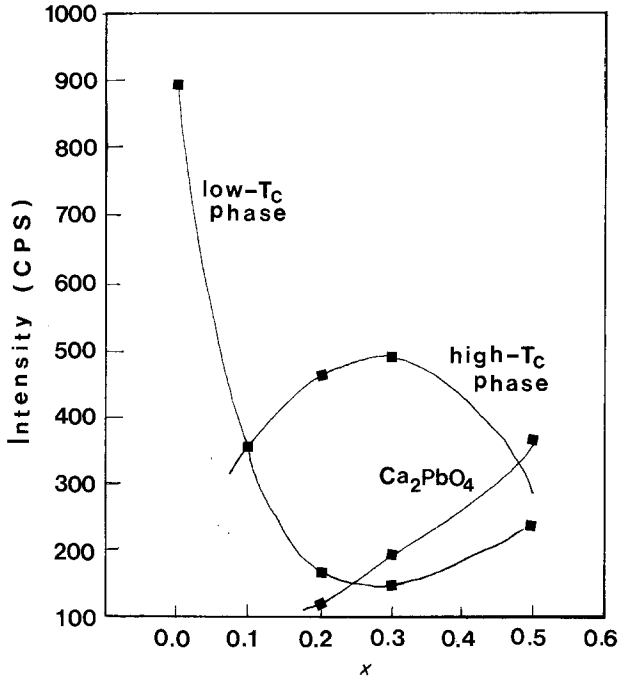

Figure 2 XRD peak intensities of (1 1 5) peaks in the low-T_c phase and high-T_c phase and (1 1 0) peaks in the Ca_2PbO_4 phase of $(Bi_{1-x}Pb_x)_2Sr_2Ca_2Cu_3O_y$.

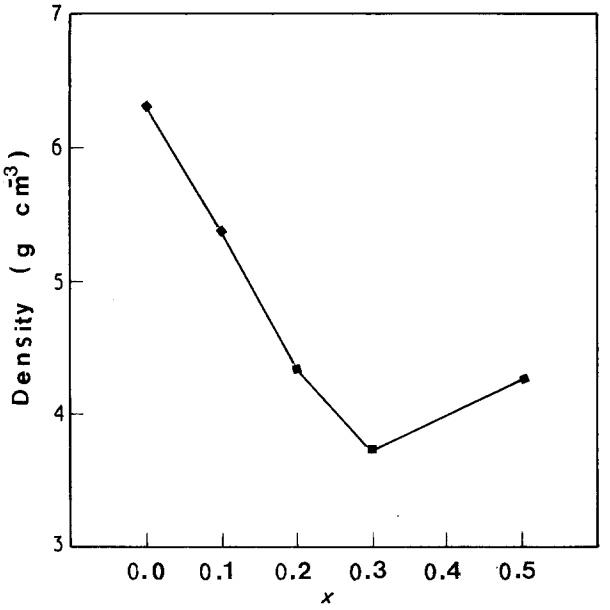

Figure 3 Apparent density versus $(Bi_{1-x}Pb_x)_2Sr_2Ca_2Cu_3O_y$ composition.

for Ca_2PbO_4, the second phase observed in the Pb-doped Bi–Sr–Ca–Cu–O system, appeared from the $x = 0.2$ composition and increased with increasing Pb doping amount. For the $x = 0.5$ composition, the Ca_2PbO_4 phase was observed to be the most dominant phase in the specimen.

Fig. 2 shows X-ray peak intensities of the (1 1 5) peaks in the low-T_c phase and high-T_c phases, and the strongest peak (1 1 0) in the Ca_2PbO_4 phase of the $(Bi_{1-x}Pb_x)_2Sr_2Ca_2Cu_3O_y$ composition. For the $x = 0.3$ composition, the strongest peak intensity of high-T_c phase was observed, while the proportion of the low-T_c phase was reduced most. On the other hand, it was observed that the high-T_c phase decreased and conversely the low-T_c phase increased for the $x = 0.5$ composition. This result can be explained through the addition of excess Pb causing excess Ca_2PbO_4 phase which suppressed the formation of the high-T_c phase.

Fig. 3 shows the apparent density change with increasing Pb addition. The density decreased with increasing Pb addition up to the $x = 0.3$ composition, and then increased for the $x = 0.5$ composition. This can be explained as due to the randomly oriented two-dimensional grain growth which is caused by the increases in the high-T_c phase and which expands the volume of the specimen. This result agrees with the variation in volume fraction of the high-T_c phase mentioned for Fig. 2.

Fig. 4 shows SEM photographs of the fracture surfaces of sintered specimens with increasing Pb addition. The grain size increases with increasing Pb addition up to the $x = 0.3$ composition. This supports the contention that the decrease of density was due to two-dimensional grain growth. However, in case of the $x = 0.5$ composition grain growth was reduced, most likely due to the suppression of formation of the high-T_c phase caused by the addition of excess Pb, and second-phase grains appear between the plate-like grains. These microstructural observations might explain the increase in density for the $x = 0.5$ composition.

Fig. 5 shows the DTA and TGA curves of the powder for the $x = 0$, 0.3 and 0.5 compositions. The

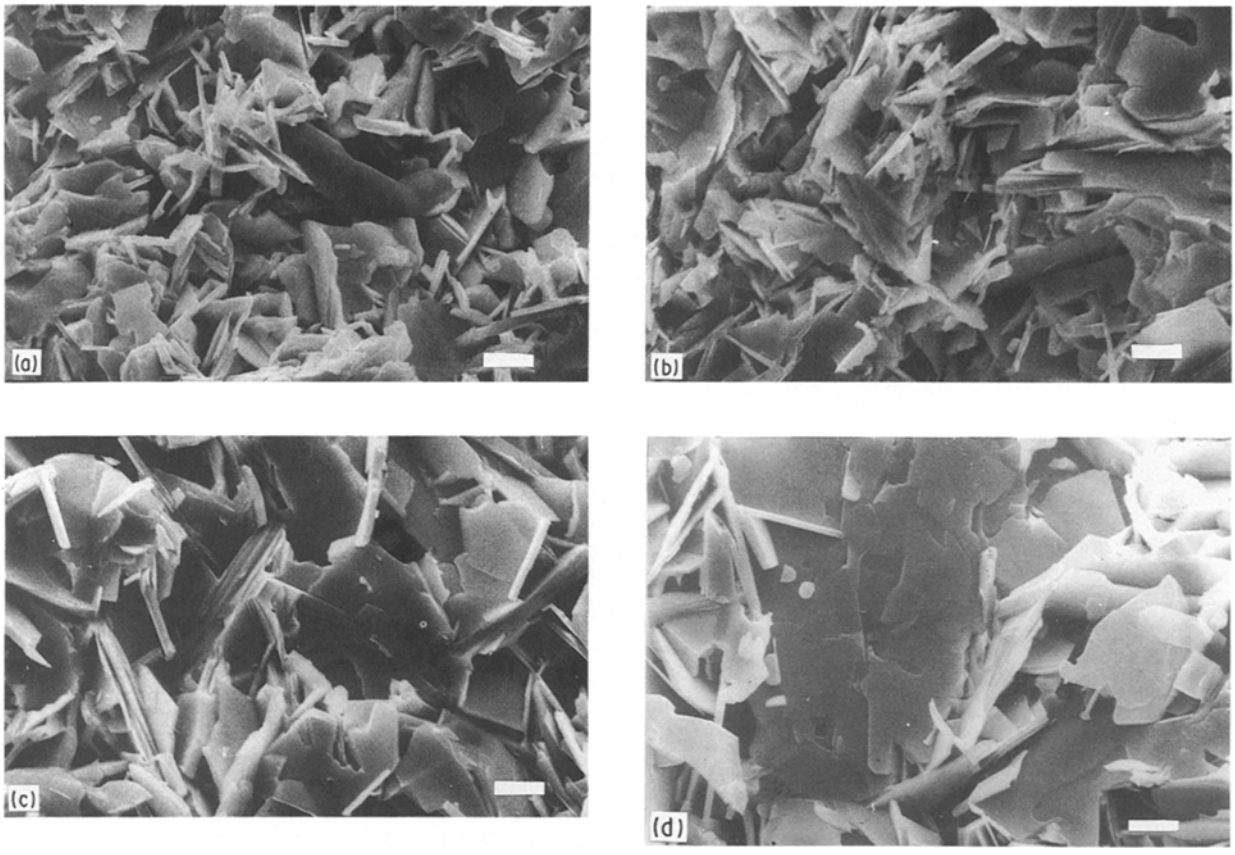

Figure 4 SEM photographs of $(Bi_{1-x}Pb_x)_2Sr_2Ca_2Cu_3O_y$: (a) $x = 0$, (b) $x = 0.1$, (c) $x = 0.2$, (d) $x = 0.3$, (e) $x = 0.5$ (fractured surface, bar = 4 μm).

high-T_c phase is produced through the low-T_c phase which was formed as an intermediate reaction product and also as a precursor of the high-T_c phase, as reported by Kijima *et al.* [13] and Hatano *et al.* [14]. We therefore made measurements on the calcined powder which contains mainly the low-T_c phase to investigate the formation process of the high-T_c phase. The large endothermic peak observed at a relatively high temperature represents the melting of the low-T_c phase. The melting point decreases with increasing Pb addition. On the other hand, the small endothermic peak observed at a relatively low temperature suggests the partial melting reported by Hatano *et al.* [14]. This was observed at 872 °C ($x = 0$), 842 °C ($x = 0.3$) and 842 °C ($x = 0.5$). This means that the partial melting occurs below the sintering temperature (845 °C) in the Pb-doped samples.

In our previous study [15], $YBa_2Cu_3O_7$ high-T_c superconductor was synthesized below the normal preparation temperature by KCl flux. The peak

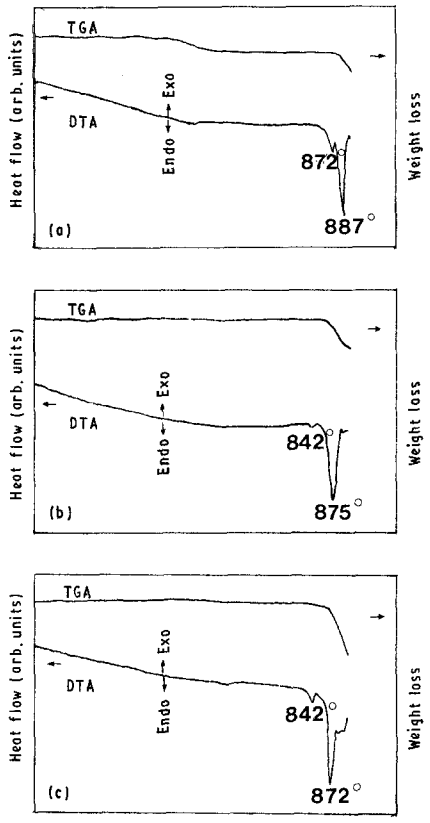

Figure 5 DTA and TGA curves for $(Bi_{1-x}Pb_x)_2Sr_2Ca_2Cu_3O_y$: (a) $x = 0$, (b) $x = 0.1$, (c) $x = 0.5$.

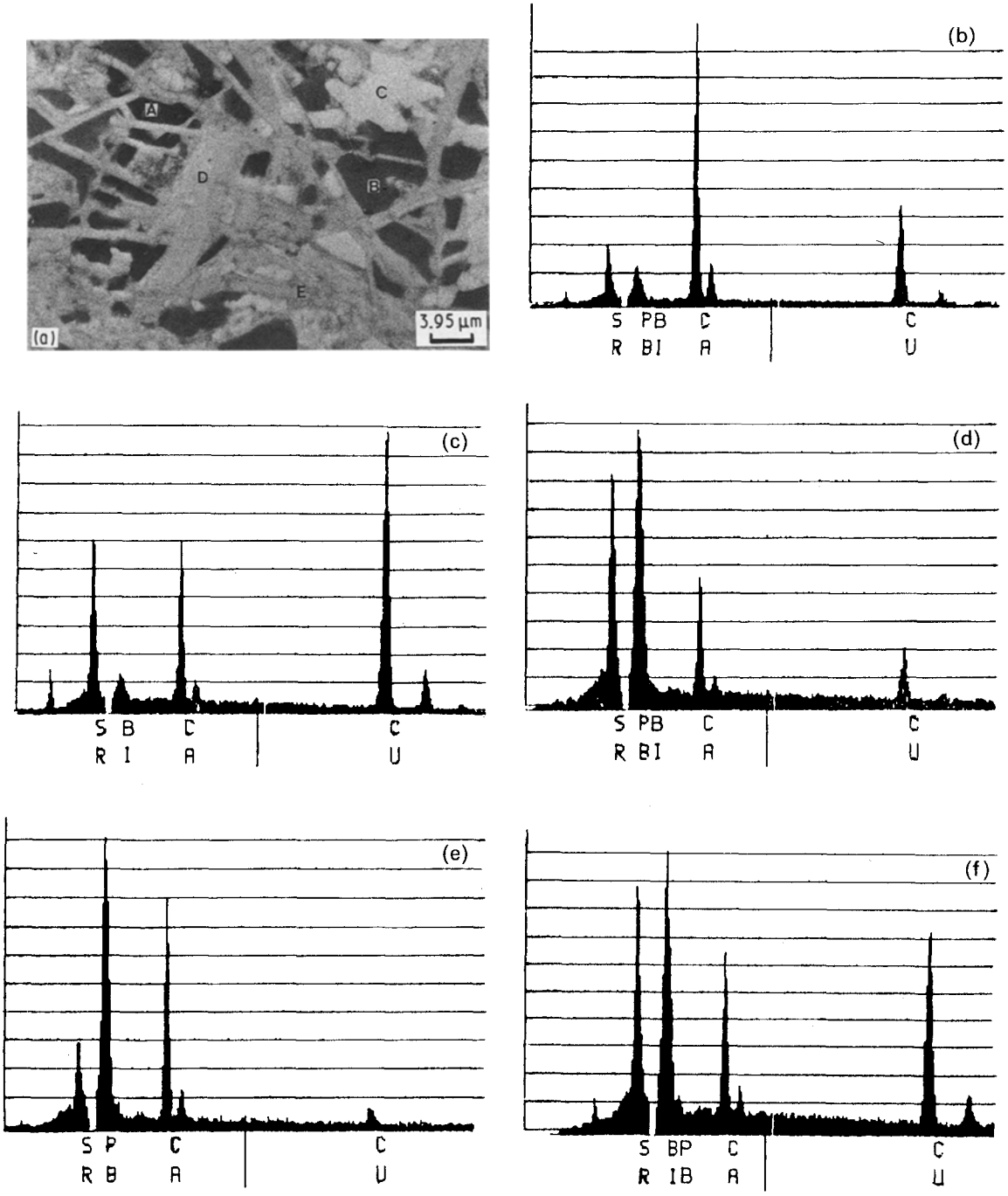

Figure 6 (a) BSE image and (b–f) EDS analysis for $(Bi_{0.5}Pb_{0.5})_2Sr_2Ca_2Cu_3O_y$: X-ray spectra of (b) phase A, (c) phase B, (d) phase C, (e) phase D, (f) phase E.

TABLE I Analysed chemical composition of phases A, B and D in Fig. 6 using SEM–EDX

Element	Composition (at %)		
	A phase	B phase	D phase
Bi	2.73	1.36	2.86
Pb	1.23	0.30	25.77
Sr	7.18	16.00	7.78
Ca	53.77	19.46	58.74
Cu	35.09	62.88	4.84

caused by the partial melting was not observed below the sintering temperature for the Pb-free composition and became larger when more Pb was added, which supports the contention that the amount of partially melted liquid phase depends on the Pb addition. Thus it is suggested that the composition of the liquid phase, caused by partial melting, appears to include a considerable number of Pb atoms, and considering that no trace of decomposition was observed in the superconducting phase after the partial melting, the partial melting might be ascribed to the effect of the second-phase component which contains Pb.

The back-scattered electron image (BSE) and EDS microanalyses for various phases in the multiphase specimen with $x = 0.5$ composition were taken to investigate the secondary phases which effect partial melting. As shown in Fig. 6, the bright region (phase C) and grey and needle-like region (phase E) seem to be the low-T_c phase and the high-T_c phase, respectively. Table I shows the atomic percentages of metallic components in the secondary phases indicated by A, B

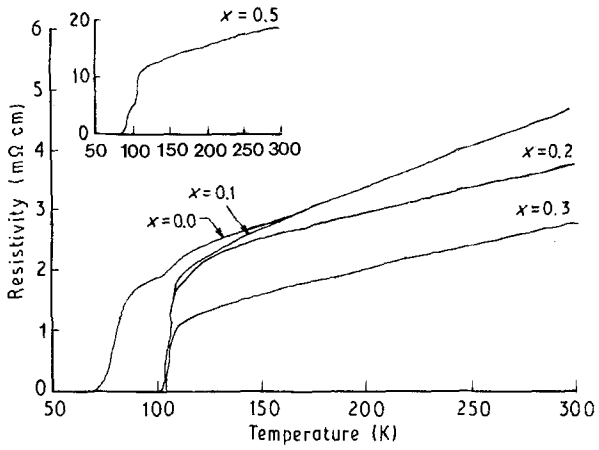

Figure 7 Temperature dependence of resistivity for $(Bi_{1-x}Pb_x)_2Sr_2Ca_2Cu_3O_y$.

and D obtained from the SEM–EDS analysis. No other impurity phases were observed in the specimen. Phase A consists mostly of Ca and Cu. According to these atomic data, the phase seemed to be Ca_2CuO_3 or a mixture of Ca_2CuO_3 and CuO. Similar results were reported elsewhere [16, 17]. Phase B consists mostly of Sr, Ca and Cu. The phase seemed to be the so-called bronze phase, which has the composition $(Sr,Ca)_3Cu_5O_8$, and many researchers [10, 18–20] have reported the existence of this phase. The peaks arising from this phase were not clearly detected in XRD measurements because of the accidental coincidence with those peaks derived from the low-T_c and high-T_c phases.

The above two phases (A and B) could be found also in the Pb-free specimen and Pb was not detected in these phases. However, phase D (the only Pb-rich secondary phase) is mainly composed of Ca and Pb. According to the atomic percentage of metallic components, this phase may be the Ca_2PbO_4 phase which has been observed in X-ray diffraction patterns for Pb-doped specimens. According to the DTA curves (Fig. 5), partial melting seems to be due to the effect of the second-phase component which contains Pb. Thus, it is thought that the secondary phase which appears to cause the partial melting is the Ca_2PbO_4 phase. As shown in Fig. 2, the Ca_2PbO_4 phase increases with increased Pb doping. It is therefore concluded that the amount of partially melted liquid phase increases with increased Pb doping, which corresponds to the result obtained from DTA measurements (Fig. 5). The melting point of Ca_2PbO_4 is 822 °C, above which it decomposes into CaO and the Pb-rich liquid phase [21]. Then the liquid phase seems to act as a flux and accelerate the diffusion to transport the constituents (including the decomposed CaO) to form the high-T_c phase. Hatano *et al.* [14] and Kijima *et al.* [13] reported that the liquid phase caused by partial melting was a Pb-rich phase. Also, magnetic susceptibility was observed at 77 K for the $x = 0$ and $x = 0.3$ compositions. The $x = 0$ composition had the value of -9.553×10^{-3} e.m.u. g^{-1} and the $x = 0.3$ composition had the value of -5.110×10^{-1} e.m.u. g^{-1}. The magnetic susceptibility observation suggests that the specimen with Pb added has a very high diamagnetic property due to the increase in the volume fraction of the high-T_c phase.

Fig. 7 shows the temperature dependence of the resistivity for the $(Bi_{1-x}Pb_x)_2Sr_2Ca_2Cu_3O_y$ composition. For the Pb-free sample, zero resistivity was not achieved above 100 K ($T_c = 70$ K), but in the case of Pb doping, T_c suddenly jumped to 101 K for $x = 0.1$, 103.5 K for $x = 0.2$ and 104 K for $x = 0.3$, but for $x = 0.5$, T_c decreased to 85 K. The normal-state resistivity decreased up to the $x = 0.3$ composition, but in the case of the $x = 0.5$ composition, the resistivity increased due to the excess semiconducting or insulating secondary phases.

4. Conclusions

1. The volume fraction of the high-T_c phase increases with increasing Pb addition up to $x = 0.3$ due to promotion of the reaction which favours high-T_c phase formation, and above that it decreases due to the promotion of the reaction favouring Ca_2PbO_4 formation.
2. The grain size is increased and density is decreased with increasing Pb addition up to $x = 0.3$, above which the grain size is decreased and density is increased due to the excess second phase.
3. Pb addition promotes formation of the high-T_c phase by the effect of Ca_2PbO_4 as a secondary phase which forms a partially melted liquid phase below the sintering temperature.

Acknowledgement

This work was supported by Yonsei University.

References

1. H. MAEDA, Y. TANAKA, M. FUKUTOMI and T. ASANO, *Jpn. J. Appl. Phys.* **27** (1988) L209.
2. A. SUMIYAMA, T. YOSHITOSHI, H. ENDO, J. TSUCHIYA, N. KIJIMA, M. MIZUNO and Y. OGURI, *ibid.* **27** (1988) L542.
3. N. KIJIMA, H. ENDO, J. TSUCHIYA, A. SUMIYAMA, M. MIZUNO and Y. OGURI, *ibid.* **27** (1988) L821.
4. H. NOBUMASA, K. SHIMIZU, Y. KITANO and T. KAWAI, *ibid.* **27** (1988) L846.
5. K. KUWAHARA, S. YAEGASHI, K. KISHIO, T. HASEGAWA and K. KITAZAWA, in Proceedings of Latin-American Conference On High Temperature Superconductivity, Rio de Janeiro, May 1988 (World Science, New Jersey, 1988).
6. U. ENDO, S. KOYAMA and T. KAWAI, *Jpn. J. Appl. Phys.* **27** (1988) L1476.
7. S. A. SUNSHINE, T. SUEGRIST, L. F. SCHNEEMEYER, D. W. MURPHY, R. J. CAVA, B. BATLOGG, R. B. van DOVER, R. M. FLEMING, S. H. GLARUM, S. NAKAHARA, R. FARROW, J. J. KRAJEWSKI, S. M. ZAHURAK, J. V. WASZCZAK, J. H. MARSHALL, P. MARSH, L. W. RUPP Jr and W. F. PECK, *Phys. Rev.* **B38** (1988) 893.
8. S. M. GREEN, C. JIANG, Yu. MEI, H. L. LUO and C. POLITIS, *ibid.* **B38** (1988) 5016.
9. R. RAMESH, G. THOMAS, S. M. GREEN, C. JIANG, YU. MEI, M. L. RUDEE and H. L. LUO, *ibid.* **B38** (1988) 7070.
10. M. TAKANO, J. TAKADA, K. ODA, H. KITAGUCHI, Y. MIURA, Y. IKEDA, Y. TOMII and H. MAZAKI, *Jpn. J. Appl. Phys.* **27** (1988) L1041.

11. A. OOTA, Y. SASAKI and A. KIRIHIGASHI, *ibid.* **27** (1988) L1445.
12. M. MATSUDA, Y. IWAI, M. TAKATA, M. ISHII, T. YAMASHITA and H. KOINUMA, *ibid.* **27** (1988) L1650.
13. N. KIJIMA, H. ENDO, J. TSUCHIYA, A. SUMIYAMA, M. MIZUNO and Y. OGURI, *ibid.* **27** (1988) L1852.
14. T. HATANO, K. AOTA, S. IKEDA, K. NAKAMURA and K. OGAWA, *ibid.* **27** (1988) L2055.
15. K. H. YOON and S. S. CHANG, *J. Appl. Phys.* **67** (1990) 2516.
16. S. ADACHI, O. INOUE and S. KAWASHIMA, *Jpn. J. Appl. Phys.* **27** (1988) L344.
17. O. INOUE, S. ADACHI and S. KAWASHIMA, *ibid.* **27** (1988) L347.
18. T. KAJITANI, M. HIRABAYASHI, M. KIKUCHI, K. KUSABA, Y. SYONO, N. KOBAYASHI, H. IWASAKI and Y. MUTO, *ibid.* **27** (1988) L1453.
19. H. KITAGUCHI, M. OHNO, M. KAICHI, J. TAKADA, A. OSAKA, Y. MIURA, Y. IKEDA, M. TAKANO, Y. BANDO, Y. TAKEDA, R. KANNO and O. YAMAMOTO, *J. Cer. Soc. Jpn* **96** (1988) 397.
20. C. J. KIM, C. K. RHEE, H. G. LEE, C. T. LEE, S. J-L. KANG and D. Y. WON, *Jpn. J. Appl. Phys.* **28** (1989) L45.
21. U. KUZMANN and P. FISHER, *Erzmetall* **27** (1974) 533.

Received 7 August
and accepted 20 December 1990